NANO LETTERS

LETTER

pubs.acs.org/NanoLett

A Single-Molecule Potentiometer

Jeffrey S. Meisner,[†,§] Masha Kamenetska,[‡,§] Markrete Krikorian,[†] Michael L. Steigerwald,[†] Latha Venkataraman,[*,‡] and Colin Nuckolls[*,†]

[†]Department of Chemistry and [‡]Department of Applied Physics and Applied Mathematics, Columbia University, New York, New York, United States

Supporting Information

ABSTRACT: Controlling electron transport through a single-molecule device is key to the realization of nanoscale electronic components. A design requirement for single molecule electrical devices is that the molecule must be both structurally and electrically connected to the metallic electrodes. Typically, the mechanical and electrical contacts are achieved by the same chemical moiety. In this study, we demonstrate that the structural role may be played by one group (for example, a sulfide) while the electrical role may be played by another (a conjugated chain of C=C π-bonds). We can specify the electrical conductance through the molecule by modulating to which particular site on the oligoene chain the electrode binds. The result is a device that functions as a potentiometer at the single-molecule level.

KEYWORDS: Nanoscale, tunneling, break-junction, oligoene, polyene, electron-transport

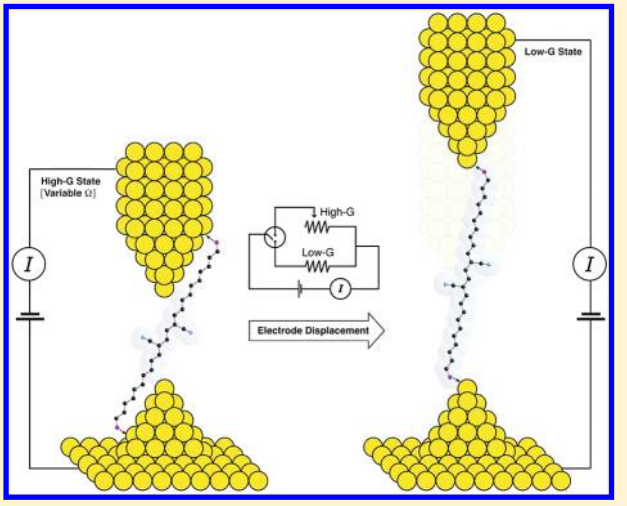

Understanding and controlling charge transport through molecular devices is critical not only to the realization of molecular-sized devices but also in advancing the performance of organic-based electronics.[1,2] For such devices, it is insufficient simply to ascertain that certain molecular backbones can conduct; one must predict, and ultimately control, molecular conductance. Here we report a new type of single-molecule electronic device in which we are able to predictably adjust the conductance of the individual molecular circuit over a well-defined range.[3] Figure 1A shows our molecule design. The terminal contact, which serves as the physical contact to anchor the molecule, is a localized, two-electron donor in the form of an organic sulfide.[4] The electrical variable-contact is the set of alternating π-bonds that form the conjugated π-space of a linear oligoene. During the conductance measurement, electronic coupling of the electrodes to the terminal contacts results in a low fixed junction conductance, while additional direct coupling through the π-space leads to higher tunable junction conductance. Furthermore, as the contact moves relative to the molecular π-space over a distance of more than 1 nm, the device conductance changes continuously. Thus we can choose a conductance for the molecule a priori simply by selecting the appropriate interelectrode spacing. These experiments form the basis for a new type of tunable molecular electronic device.

For this study, we designed and synthesized two series of molecular wires that are atomically defined segments of polyacetylene,[5,6] each with different terminal anchor groups (**A***n* and **B***n* in Figure 1A). A simple synthesis was developed that affords molecules longer than 4 nm. This synthesis also tolerates a diversity of end groups while the cyano-groups on the molecular backbone enhance molecular stability due to lowered HOMO and LUMO energies relative to vacuum (see Supporting Information). The crystallographically determined molecular structures of the parent series (**D***n*) show an ideal path of conjugation with alternating single and double bonds exclusively in the trans configuration (see Supporting Information Figure S1). The color of these compounds is a strong function of the molecular length, indicating that the HOMO−LUMO gap in these molecules decreases with increasing molecular length (see Supporting Information Figures S2−S4).

We first demonstrate that these oligoenes behave as molecular wires by measuring their electrical properties using a scanning tunneling microscope-based break-junction technique.[7] Using a gold STM tip and substrate, Au−Au point-contacts are repeatedly formed and broken to expose undercoordinated Au atoms on the electrodes. This technique is performed in a dilute solution of the target oligoene (10 μM in 1,2,4-trichlorobenzene), trapping oligoenes between the gold electrodes.[8] We apply a constant bias voltage (ranging between 200 and 750 mV)[9] and measure the current that passes between the two gold electrodes. When oligoenes bridge the broken point-contacts, we measure the conductance of these Au−oligoene−Au junctions as a function of the distance between the two electrodes.

Received: December 17, 2010
Revised: February 15, 2011

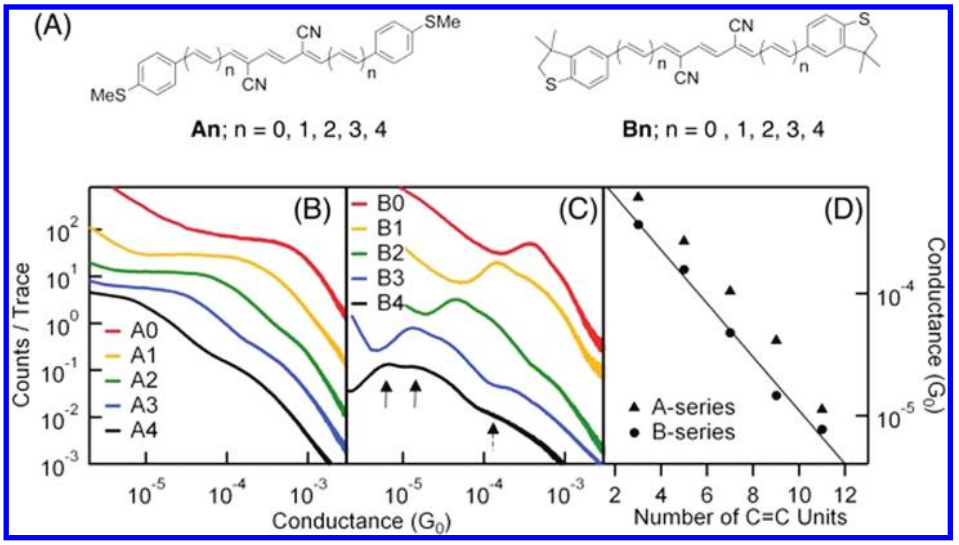

Figure 1. (A) Chemical structure of oligoene families **A***n* and **B***n*. (B,C) Linear histograms generated without data selection from >5000 conductance traces collected in the presence of each of the **A***n* and **B***n* molecules, respectively. Traces have been offset vertically for clarity. The **B***n* series show clear peaks at molecule-specific conductance values, indicated by the solid arrow for **B**4. In the longer molecules, a shoulder at higher conductance is visible, indicated by the dashed arrow for **B**4. (D) Peak positions of the single-molecule conductance peaks observed for the **A***n* and **B***n* series as a function of the total number of oligoene units. For the **A***n* series the peak position was taken from the logarithmic histograms (see Supporting Information Figure S3). A linear fit to the data on the semilog plots reveals that in both cases, conductance decays exponentially with a decay factor β of 0.22/Å.

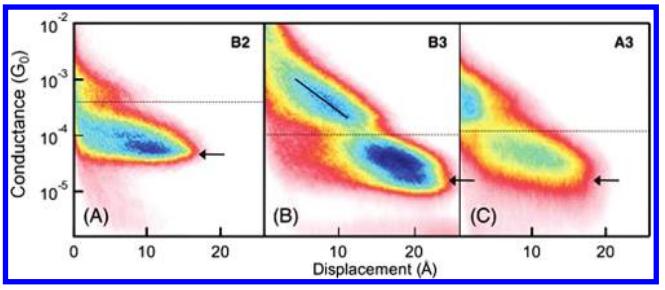

Figure 2. The 2D conductance histograms preserve displacement information for (A) **B2**, (B) **B3**, and (C) **A3** respectively. Comparing (A) and (B) within the same linker-family, longer molecules are able to sustain more junction elongation while remaining bound in the junction. All three molecules show a higher conductance shoulder in the region above the dashed line, corresponding to a junction geometry that forms immediately after rupture of the Au−Au contact. The average slope of this high conductance shoulder (solid line) reveals that conductance in this geometry decays with $\beta \sim 0.2$/Å as the junction is stretched, which is in agreement with the decay constant shown in Figure 1D. Arrows indicate peak positions in from conductance histograms in Figure 1C.

The data are recorded in the form of conductance traces (see Supporting Information Figure S5). Measurements are repeated thousands of times and conductance histograms are constructed without any data selection to reveal statistically significant conductance values (see Figure 1B,C). Oligoenes that bind to undercoordinated Au during these measurements though the methylsulfide-terminated series, **A***n*, show a broader distribution of conductances than the cyclic analogues, **B***n*. The main reason for a broad peak is a result of the additional rotational freedom around the aryl−sulfur bond, which increases the junction-to-junction variation.[10] When measuring thousands of junctions, the electrode geometry constrains the Au−S−aryl bond angles differently for different junctions resulting in a larger distribution of conductances. However, the general trends within and between the two sets are similar; incorporation of the linking sulfur atom into the five-membered ring does not significantly alter the fundamental physics, though it simplifies the analysis.

Within each series, the peak in the conductance histograms (arrow positions in Figure 1) decays exponentially with increasing length, following the expected relation, $G \sim e^{-\beta n}$ (Figure 1D). The decay constant, β, is 0.22/Å for the **B***n* series, which is in agreement with previously published values for conjugated molecules.[11] Typically, histograms show a single conductance peak; however, for $n > 1$ **A***n* and **B***n*, in addition to the conductance peaks indicated by arrows in Figure 1C, we see a second broad increase in counts at significantly higher conductance values (dashed arrow in Figure 1C). To elucidate these two conductance regions, we examined two-dimensional (2D) conductance histograms,[12,13] which preserve displacement information during junction elongation. In Figure 2, we show 2D histograms for **B2**, **B3**, and **A3**, where two regions with increased counts are clearly seen (separated by the dashed line for clarity). The higher conductance region forms immediately following the breaking of a Au-to-Au point-contact (at zero-displacement in this 2D histogram). The extent to which this high-conductance state persists as the junction extends depends on *n*, as well as the terminal group (see Supporting Information Figures S6 and S7). In Figure 2B, we see also that the value of the conductance in this high-conducting state decreases almost exponentially as the gap widens. Furthermore, this high-conductance region is absent in the shortest molecules.

One possibility for the two different conductance regimes is that these all-trans oligoenes may access two different conformations: the s-cis and s-trans. As the junction is elongated, oligoenes undergo rotations around the C−C single bonds. However, the two conformers are expected to have similar conductance; thus, rotational isomerization cannot explain this finding.[14]

We postulate instead that there are two independent conductance pathways. In the higher conductance state the tunneling path originates at one electrode, passes directly to the olefin backbone,

dx.doi.org/10.1021/nl104411f |*Nano Lett.* XXXX, XXX, 000–000

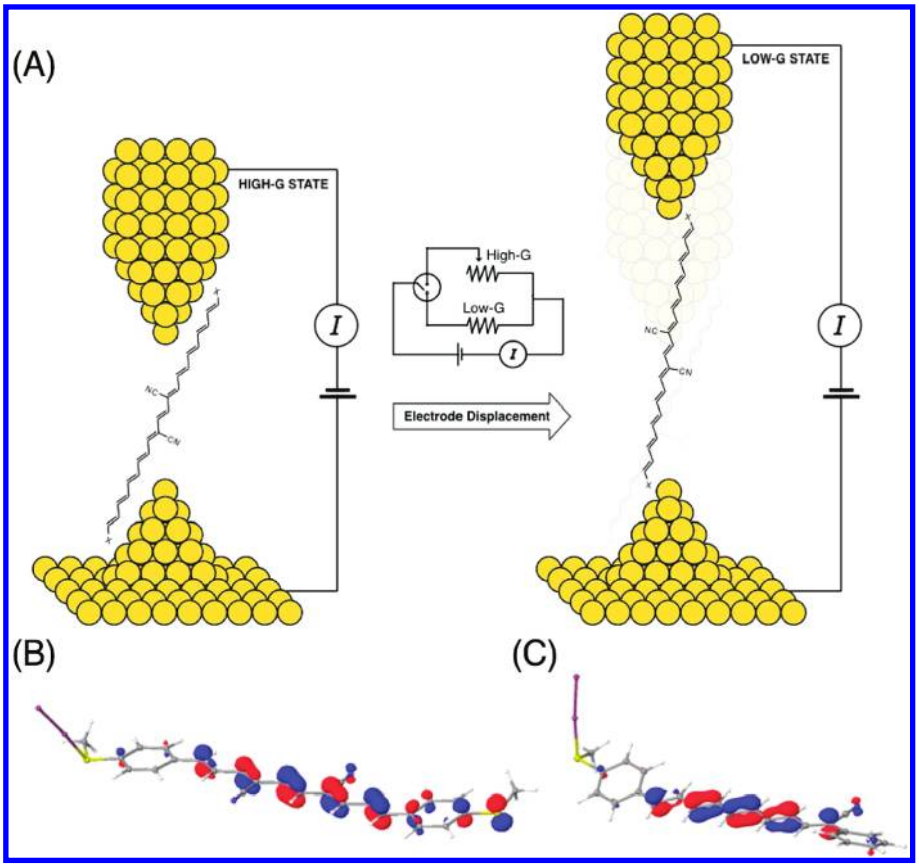

Figure 3. (A) Schematic depiction of an oligoene break junction. Both the polyolefin chain and the end groups, X, may act as electrical contacts. Oligoenes behave as a resistive potentiometer as the tip displaces along the olefin backbone, while the alkylthio end groups stabilize the junction. DFT calculations produce the HOMO of (B) Au_2-**A1** and (C) Au_2-**C4** complexes, respectively. The HOMO shows significant electron density both along the polyolefin chain and at the terminal methylsulfide functional group.

hence via the sulfide to the second electrode, as illustrated in Figure 3A. In the lower conductance state, which occurs only when interelectrode distances are sufficiently large, the tunneling path switches from electrode−olefin−sulfide−electrode to the more typical electrode−sulfide−olefin−sulfide−electrode. Although both terminal alkylthio groups anchor the oligoene to the electrodes, close proximity of the electrode to the olefin backbone results in a low-resistance pathway (high-conductance state) directly from the electrode to the olefin backbone. As the junction is extended further, it slides up the backbone until an abrupt change in conductance is observed. Once fully extended, the oligoene is bound at the apex of each electrode, where Au atoms are no longer in proximity to the polyolefin chain, and the high-conductance state turns off. The lower conductance at this stage corresponds to the conductance through the entire molecule, and follows an exponential decay with increasing molecule length (β = 0.2/Å; see Figure 1D). Extending the junction further breaks the molecular circuit, and conductance is lost.

For the longer molecules (for example, for **B3** and **B4**), as we extend the electrodes we see the conductance decay by ~0.2/Å in the high-conductance state (Figure 4). This high-conductance state is observed directly after breaking the Au point-contact where electrode separation is about 6−7 Å.[15,16] This distance is significantly smaller than the molecular lengths of **B3** and **B4**, whose lengths are 32.6 and 37.4 Å, respectively. Although the high-conductance state could be explained by assuming that the molecules are bound to the apex of the electrodes at an angle that increases with junction elongation,[23] our experimental results do not support this model for the following reasons. First, for **B3** and **B4**, the binding angle, θ, would range from about 80 to 40°, given the long molecular length and short electrode separation. Within this range of angles, we do not see the conductance decrease with increasing θ following a $(\sin \theta)^4$ dependence.[23] Second, we do not see the high-conductance state for the short molecules. If the molecules were indeed binding between the apexes of the electrodes at an angle, an angle-dependent conductance should have been observed for all molecules studied. Finally, the decay constant seen in the high-conductance state is very close to that seen for the molecular series studied, consistent with a model where the high-conductance state results from direct tunneling from the electrode to the olefin backbone.

For the shortest molecules in our study, the length of the olefin chain is comparable to the distance between electrodes upon Au−Au point-contact rupture (6−7 Å).[15,16] Thus direct contact between the electrode and the polyolefin backbone is rarely accommodated. As a result, no clear high-conductance peak is seen in Figures 1B and C (or in Supporting Information Figures S6 and S7). Other factors such as steric hindrance and the electron-withdrawing properties of the nitriles may result in only one conductance value.

To dismiss the possibility that the Au binds through the nitrile groups on the backbone, we synthesized an oligoene analogous to **A1**, but lacking nitriles. For this molecule, we observe the two-conductance states as well, indicating that the nitriles are not responsible for this two-state behavior (see Supporting Information

dx.doi.org/10.1021/nl104411f |*Nano Lett.* XXXX, XXX, 000–000

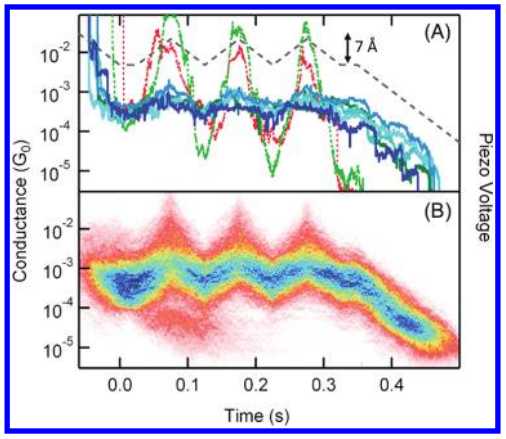

Figure 4. (A) Sample traces collected in the presence of **B4** (solid blue), 1,6-bis(methylsulfide)hexane (dashed red), and only clean solvent (dashed green). Traces with **B4** show conductance changing continuously and reversibly as the piezo voltage is modulated along the dashed black line so that the junction is repeatedly stretched and compressed. (B) A 2D histogram constructed from selected traces for which the average conductance during the initial hold section fell within the high-conductance range. More than 50% of the 3000 traces collected met the selection criteria. Fitting the average slope of the different sections of the piezo ramp shows that the conductance grows and decays exponentially with a factor of 0.2/Å throughout the measurement, emphasizing the reproducibility of the potentiometer behavior.

Figure S8). In fact, the enhanced high-conductance state in this molecule compared to **A1** suggests that the absence of the nitriles facilitates greater coupling of the olefin to the electrode by removing some steric hindrance, as well as making the olefin more electron rich (see Supporting Information Figures S4 and S8).

While both S—Au and olefin—Au bonds form, it is clear that the former is stronger than the latter. We demonstrate the importance of this with a series of asymmetric oligoenes, each having only one sulfide (**C***n*), and with another series that lacks sulfides entirely (**D***n*) (see Supporting Information Figure S8). None of the **D***n* examples tested showed a measurable conductance, while the **C***n* series showed conductances that are measurable, albeit quite low. Moreover, the absolute height of the peak in the conductance histogram for **C***n* is quite low, suggesting that the formation of an Au—**C***n*—Au junction is a lower probability event. Thus the π-complex is not strong enough to hold the mechanical circuit together alone, but if the molecule is held in the junction by at least one strong structural element, the π-complex link is strong enough to complete the electrical circuit.

To further explore this unusual mode of electrode—molecule coupling, we turned to computation. Density functional theory (DFT) calculations (B3LYP/6-31G**) on **A1** allowed us to clearly visualize the molecular orbitals (MOs) pertinent to molecular junction formation (see Supporting Information for details). We modeled this as a two-step process; the molecule first binds to one electrode, and then this electrode—molecule complex binds to the second electrode. This model elucidates the different modes of binding to the second electrode that are available to the molecule as the gap between the two electrodes changes. For conceptual as well as computational simplicity, we chose to model the Au electrode with diatomic Au_2.[17] In Figure 3B, we show the HOMO calculated for the optimized geometry of Au_2—**A1,** in which the Au_2 unit is bound to one of the terminal sulfides. Examination of these MOs suggests that oligoenes contain two potential electrode-binding locations; not only at the distal SMe, but also along to the π-system of the polyolefin backbone. Both binding locations have ample precedent in homogeneous organometallic chemistry[18] and would result in different electron tunneling pathways. Thus these calculations are consistent with our observations that **A***n* and **B***n* show two conductance states. Previous reports reveal that it is common for transition metals to interact with oligoenes. In addition to the numerous weak and dynamic interactions between transition metals and alkenes, stable inorganic complexes have been isolated, in which Pd and Ru interact directly with oligoenes through the π-system.[19−21] For comparison, in Figure 3C we show the HOMO for **C4**. This orbital is essentially entirely in the π-space of the oligoene. Thus the channel for electrical conduction is present in **C4**, and it is quite similar to the channel in the **A***n* and **B***n* series. The difference in the conductances of **A1** (and **B1**) versus **C4** lies in the ability of the sulfide to hold the molecule physically close to the metal electrode, rather than in the electronic structure of the molecular conductor.

If we indeed have a direct conduction path from the electrode through the olefin backbone, it should be possible to change the conductance by modulating the electrode position and generating a single-molecule circuit that functions as a potentiometer. This is shown in Figure 4. Here, conductance is measured in a solution of **B4** while applying a modified ramp to our piezoelectric actuator, which controls the substrate position relative to the fixed tip[22] (see Figure 4A, dashed trace). Of the 3000 traces measured with this ramp, over 50% of the traces show a molecule in the high-conductance regime at the start of the zigzag ramp, as determined by an automated algorithm. A sample of selected traces is shown in Figure 4A, and all selected traces were used to construct the 2D conductance-time histogram on a semilog scale, shown in Figure 4B. The conductance follows a zigzag pattern, as the tip—sample distance is modulated by 7 Å, with an average change in conductance from $\sim 4 \times 10^{-4}$ G_0 to $\sim 2 \times 10^{-3}$ G_0. This range is within the high-conductance regime for this molecule, and has an exponential dependence on separation ($e^{-0.2/\text{Å}}$). An exponential dependence of conductance on electrode distance suggests that while the contact resistance does not change the length of the backbone through which transport occurs varies as the junction is compressed or elongated. Control experiments with alkanes show no modulation of conductance (Figure 4A). Traces collected in pure solvent show changes in conductance between 10^{-6} G_0 to 10^{-1} G_0 during the zigzag ramp, which would be expected for tunneling through a gap without molecules. The ability to change the conductance of the junction continuously in this high-conductance state with an exponential decay of 0.2/Å can only be explained if the contact to the molecule is through direct π-coupling to the electrodes.

In conclusion, we experimentally demonstrate transport through single-molecule junctions where direct electronic coupling between the molecular π-conjugated backbone and Au electrode is achieved. Furthermore, this coupling is enabled by an auxiliary terminal chemical linker that provides mechanical support for the junction. Conductance through the molecular backbone can be tuned continuously and reversibly by changing the electrode separation. Thus, this system provides a new class of molecular scale devices that perform as a resistive potentiometer.

■ ASSOCIATED CONTENT

Supporting Information. Chemical structures, synthetic experimentals, and UV—vis absorption spectroscopy for **An, Bn**, **C***n*, and **D***n*; cyclic voltammetry; STM break junction experimental conditions and controls; and theoretical methods and

dx.doi.org/10.1021/nl104411f |*Nano Lett.* XXXX, XXX, 000–000

details. This material is available free of charge via the Internet at http://pubs.acs.org.

AUTHOR INFORMATION

Corresponding Author

*E-mail: (L.V.) lv2117@columbia.edu; (C.N.) cn37@columbia.edu.

Author Contributions

§These authors contributed equally to this study.

ACKNOWLEDGMENT

This work was supported in part by the Nanoscale Science and Engineering initiative of the NSF (Award CHE-0641523) and the New York State Office of Science, Technology. L.V. thanks the Packard Foundation for support. This research was also funded by the Chemistry Research Instrumentation and Facilities: Multiuser program (CRIF:MU) of the National Science Foundation (Award Number 0840451), the Chemical Sciences, Geosciences. and Biosciences Division Office of Basic Energy Sciences, U.S. DOE (DE-FG02-01ER15264), and as part of a National Science Foundation Center for Chemical Innovation (CCI Phase 1 - Award Number CHE-0943957).

REFERENCES

(1) Nitzan, A.; Ratner, M. A. *Science* **2003**, *300* (5624), 1384–1389.

(2) Joachim, C.; Ratner, M. A. *Proc. Natl. Acad. Sci. U.S.A.* **2005**, *102* (25), 8800–8800.

(3) Lafferentz, L.; Ample, F.; Yu, H.; Hecht, S.; Joachim, C.; Grill, L. *Science* **2009**, *323* (5918), 1193–1197.

(4) Park, Y. S.; Whalley, A. C.; Kamenetska, M.; Steigerwald, M. L.; Hybertsen, M. S.; Nuckolls, C.; Venkataraman, L. *J. Am. Chem. Soc.* **2007**, *129* (51), 15768–15769.

(5) Knoll, K.; Krouse, S. A.; Schrock, R. R. *J. Am. Chem. Soc.* **1988**, *110* (13), 4424–4425.

(6) Catalan, J.; Hopf, H.; Mlynek, C.; Klein, D.; Kilickiran, P. *Chem.—Eur. J.* **2005**, *11* (13), 3915–3920.

(7) Xu, B. Q.; Tao, N. J. J. *Science* **2003**, *301* (5637), 1221–1223.

(8) Venkataraman, L.; Klare, J. E.; Nuckolls, C.; Hybertsen, M. S.; Steigerwald, M. L. *Nature* **2006**, *442* (7105), 904–907.

(9) This bias range was required to measure conductances down to 10^{-6} G_0. No bias dependence was found within this bias range.

(10) Park, Y. S.; Widawsky, J. R.; Kamenetska, M.; Steigerwald, M. L.; Hybertsen, M. S.; Nuckolls, C.; Venkataraman, L. *J. Am. Chem. Soc.* **2009**, *131* (31), 10820–10821.

(11) He, J.; Chen, F.; Li, J.; Sankey, O. F.; Terazono, Y.; Herrero, C.; Gust, D.; Moore, T. A.; Moore, A. L.; Lindsay, S. M. *J. Am. Chem. Soc.* **2005**, *127* (5), 1384–1385.

(12) Quek, S. Y.; Kamenetska, M.; Steigerwald, M. L.; Choi, H. J.; Louie, S. G.; Hybertsen, M. S.; Neaton, J. B.; Venkataraman, L. *Nat. Nanotechnol.* **2009**, *4* (4), 230–234.

(13) Martin, C. A.; Ding, D.; Sorensen, J. K.; Bjornholm, T.; van Ruitenbeek, J. M.; van der Zantt, H. S. J. *J. Am. Chem. Soc.* **2008**, *130* (40), 13198–13199.

(14) The rotational barrier about the single bond in a conjugated diene is ~6 kcal/mol, where the local minima of the s-cis conformer lies ~2 kcal/mol higher in energy (seeCarriera, L. A. *J. Chem. Phys.* **1975**, *62* (10), 3851–3854). Time-dependent DFT calculations on a **D3** (all s-trans) estimates the rotation about the a single bond at 4 kcal/mol. Calculations suggest that orbitals energies of these conformers are similar and also that molecular length is does not change significantly before and after rotation The s-trans/s-cis conformers are not expected to account for the dramatic difference between the high- and low-conductance states in our break junction measurements but may contribute to peak broadening.

(15) Yanson, A. I.; Bollinger, G. R.; van den Brom, H. E.; Agrait, N.; van Ruitenbeek, J. M. *Nature* **1998**, *395* (6704), 783–785.

(16) Kamenetska, M.; Koentopp, M.; Whalley, A.; Park, Y. S.; Steigerwald, M.; Nuckolls, C.; Hybertsen, M.; Venkataraman, L. *Phys. Rev. Lett.* **2009**, *102* (12), 126803.

(17) We chose to model the Au electrode by using the simplest possible local model, the homonuclear diatomic cluster, Au_2. This model offers the empty orbital space (Lewis acidity) into which the S lone pair can delocalize to form the donor−acceptor bond that initiates the molecular-bridge-forming process.

(18) Collman, J. P.; Hegedus, L. S.; Norton, J. R.; Finke, R. G. *Principles and Applications of Organotransition Metal Chemistry*; University Science Books: 1987.

(19) Fukumoto, H.; Mashima, K. *Organometallics* **2005**, *24* (16), 3932–3938.

(20) Fukumoto, H.; Mashima, K. *Eur. J. Inorg. Chem.* **2006**, *24*, 5006–5011.

(21) Murahashi, T.; Mochizuki, E.; Kai, Y.; Kurosawa, H. *J. Am. Chem. Soc.* **1999**, *121* (45), 10660–10661.

(22) Xia, J. L.; Diez-Perez, I.; Tao, N. J. *Nano Lett.* **2008**, *8* (7), 1960–1964.

(23) (a) Haiss, W.; Wang, C.; Grace, I.; Batsanov, A. S.; Schiffrin, D. J.; Higgins, S. J.; Bryce, M. R.; Lambert, C. J.; Nichols, R. J. *Nat. Mater.* **2006**, *5*, 995–1002. (b) Kornilovitch, P. E.; Bratkovsky, A. M. *Phys. Rev. B.* **2001**, *64*, No. 195413.